

# Material hybrid joining of sheet metals by electromagnetic pulse technology

Ralph Schäfer<sup>1, a</sup>, Pablo Pasquale<sup>1, b</sup>

<sup>1</sup>PSTproducts GmbH, Junkersstr. 163755 Alzenau, Germany

**Keywords:** Electromagnetic forming, welding, material hybrid atomic joining.

**Abstract.** Adhesively joining metals of dissimilar melting point represents one of the most sophisticated tasks in joining technique. However, due to light weight considerations this type of joint, for example the connection between an aluminum flange and a high strength steel crash element, is of prior interest. The electromagnetic pulse technology is a proven process to accomplish adhesive joints between tubes made of dissimilar metals. Recent developments of the technique now allow welding even dissimilar and similar sheet metals under industrial conditions. This paper details the underlying mechanisms and shows a variety of samples, depicting for the potential of this new process.

## Introduction

Fusion welding processes are widely adopted within production technology. However, these processes are not capable for joining metals of strongly different melting points. For example Aluminum melts at temperatures above 660°C [1], whereas iron melts at temperatures 1536°C [2]. Because of this large melting point discrepancy the creation of a aluminum-steel weld puddle is hindered [2]. Moreover, during solidification brittle intermetallic phases will be generated, which will significantly decrease the mechanical properties of the joining area [2,3].

Hence, adhesive joining of aluminum to steel is best possible, if none or at least only one of the joining partners is melted. In general, there are two ways to accomplish that, solid phase welding (friction/ friction stir welding, explosion welding) and by a combination of welding and brazing, where the aluminum is melted, but the steel not. The welding/ brazing combination tends to produce some intermetallics [3]. Solid phase welding normally does not create intermetallics [4]. For joining sheet material friction stir welding is applicable, but the welding velocity is only in the range of 1m/min and the process demands for quite small tolerated gaps between both contact partners [5]. A new possibility to manufacture high quality joints even between steel and Aluminum sheets is given by the electromagnetic pulse technology (EMPT). The process is based on the same principle as explosion welding, only the explosive is replaced by a fully controllable, pulsed electromagnetic field. Hence, EMPT sheet welding systems can be operated without any danger for production personal within normal production lines.

## Fundamentals of the electromagnetic pulse technology

**Electromagnetics:** In 1831, Michael Faraday and Joseph Henry measured transient voltages at electrical conductors in time varying magnetic fields. This phenomenon is called electrical induction [6]. An electrical conductor, loaded by a time varying current is capable to produce transient magnetic field. Hence, a wire, loaded by a transient current inducts current in neighboring conductors. Lenz's rule states that inducted currents oppose their origin. If two neighboring wires are loaded by currents of opposing direction, a repelling mechanical force will be established between those conductors. EMPT takes benefit of these principles: An electrical coil, neighboring one of the both sheet to be joined, is loaded by a strong, but pulsed current. The magnetic field, generated by this current inducts eddy currents, running at the surface of the workpiece in opposite direction to the coil current. A repelling force is generated, see Fig. 1.

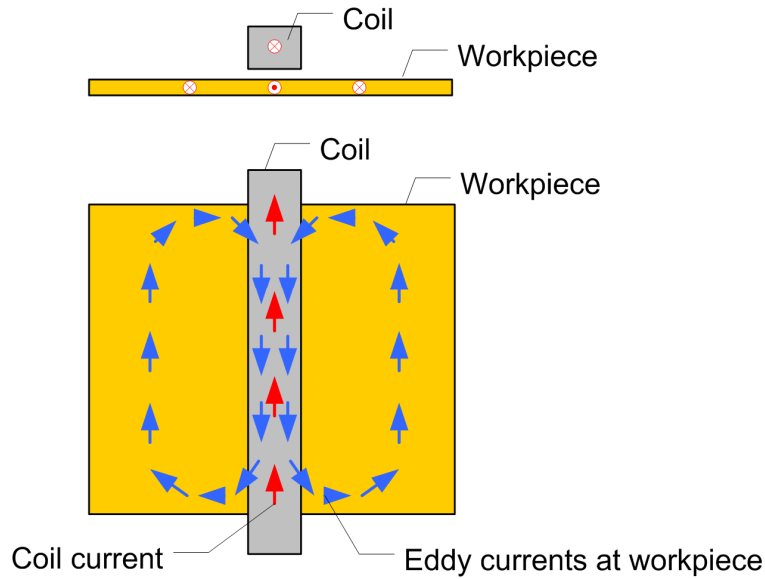


Fig. 1: Induced currents with respect to EMPT sheet welding

**Mechanics:** The coil current and the eddy current at the workpiece surface repel each other. When the magnetic field is strong enough to overcome the workpiece yield strength and inertial effects, partial plastic deformation of the sheet metal takes place (Fig. 2:  $t_1$ ). Prior to the impact on the joining partner the deformed geometry is shaped like a bulge. The first contact between the accelerated sheet, the so called flyer, and its stationary contact partner takes place in the area of the bulge head. Due to the geometric situation, the contact zone is line-shaped (Fig. 2:  $t_1$ ). Only contact normal stress loads this line. At both sides of this contact line V-shaped gaps can be seen. In the ongoing process, the V-shaped gaps will close, i.e. the flattening of the bulb evolves (see fig 2:  $t_2$ ,  $t_3$ ). During the closure of the V-shaped gaps, the contact loading condition changes from pure normal stress within the first line contact to a combination of contact normal stress and tangential stress at later stages of the process. Table 1 gives maximum velocity and contact stress probe values for five points within the contact zone. The second column depicts for the time interval between the contact of the bulge tip (point #1) and the first contact closure of the respective point. The location of these probe points is given in fig. 2,  $t_3$ . For the flyer and the static contact partner material data representing Al 6060 T4 are used. The wall thickness for both contact partners is 1mm.

| Point # | Time after first impact [ns] | Tangential velocity [m/s] | Normal velocity [m/s] | Contact tangential stress [N/mm <sup>2</sup> ] | Contact normal stress [N/mm <sup>2</sup> ] |
|---------|------------------------------|---------------------------|-----------------------|------------------------------------------------|--------------------------------------------|
| 1       | 0                            | 0                         | 396                   | 0                                              | 2700                                       |
| 2       | 250                          | 179                       | 395                   | 70                                             | 2800                                       |
| 3       | 550                          | 471                       | 471                   | 260                                            | 6500                                       |
| 4       | 1000                         | 723                       | 558                   | 190                                            | 4700                                       |
| 5       | 1750                         | 520                       | 230                   | 25                                             | 4700                                       |

Table 1: Velocities and contact stresses at the time of impact for five interfacial points

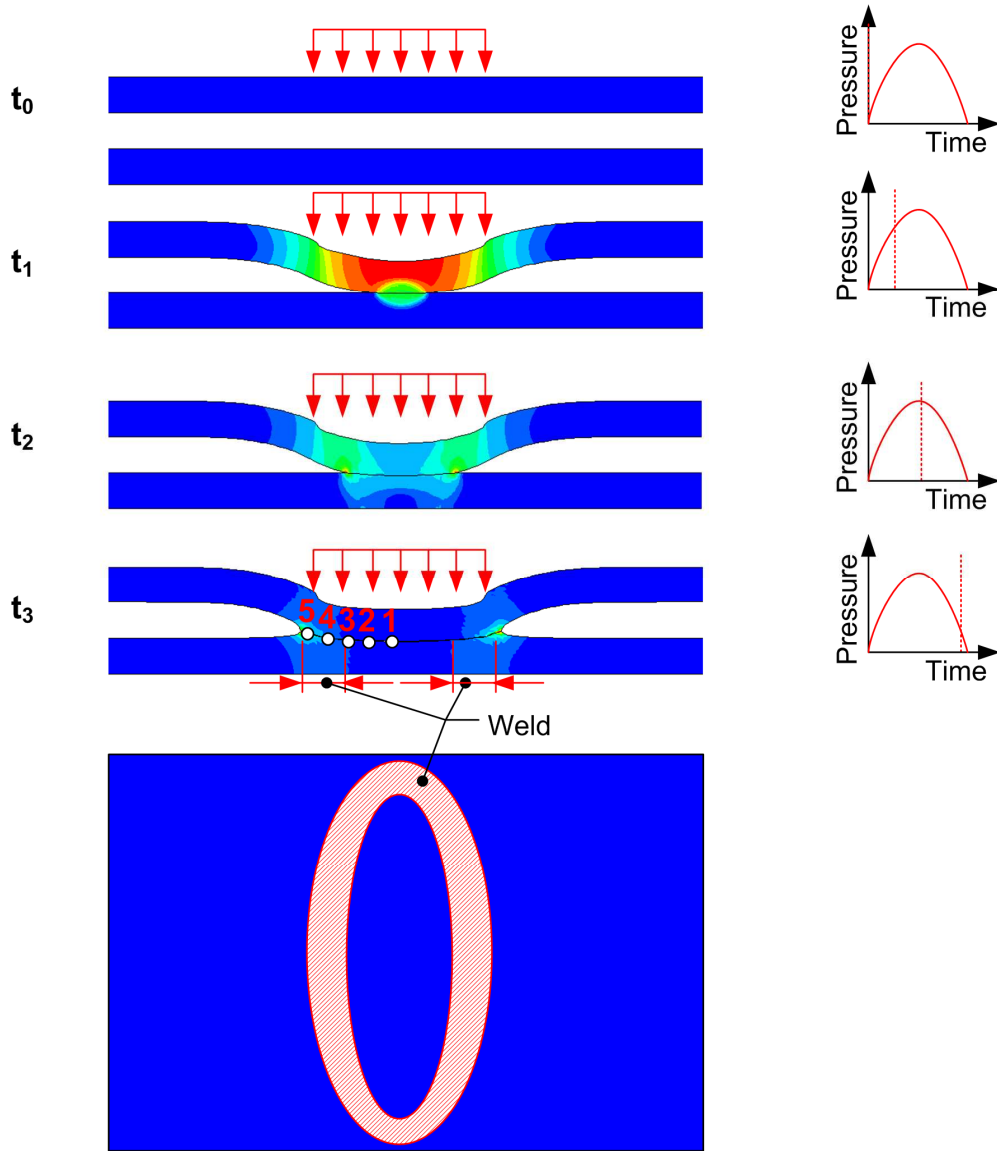


Figure 2: Kinematics of the EMPT sheet welding process

Evidently, the impact velocity components as well as the contact normal stress increases during the impact process; point #3 marks the area of highest amplitudes. After that, the stress and velocity values decrease until point #5, which is the end of the welding area. The strong velocity increase is due to energy conservation. The kinetic energy just before impact is decreased by energy essential for further plastic yielding of the flyer and energy losses due to plastic deformation of the static contact partner. The flattening of the bulge starts at point 1. Sequentially, the points 2 to 5 will come in contact, i.e. the flyer velocity decreases to zero when the respective point comes in contact with the contact partner. The equation of energy conservation is given by eq.1:

$$E_{\text{kinetic\_flyer}} - E_{\text{plastic\_flyer}} - E_{\text{plastic\_stator}} = 0. \quad (1)$$

For instructive purposes it is helpful to model the flyer just by a chain of points, where a mass  $m$  and a velocity  $v$  is associated to each point  $i$ . The kinetic energy of the flyer is then given by

$$E_{\text{kinetic\_flyer}} = \frac{1}{2} \sum m_i v_i^2. \quad (2)$$

During the bulge flattening subsequently points of the chain loose their velocity during impact. If the energy consumption for plastic yielding of the flyer and the stator is lower than the energy of the

stopped point at the time of impact, the principle of energy conservation demands for a velocity increase in the adjacent points. Fig. 3 represents the time- velocity curves for the five points illustrated in fig. 2. The velocity data emphasize that point 3 gains significant velocity directly after impact of point 2. Point 4 accelerates strongly after impact of point 3. The acceleration of point 5 is strongly damped by the plastic deformation of the flyer in that zone.

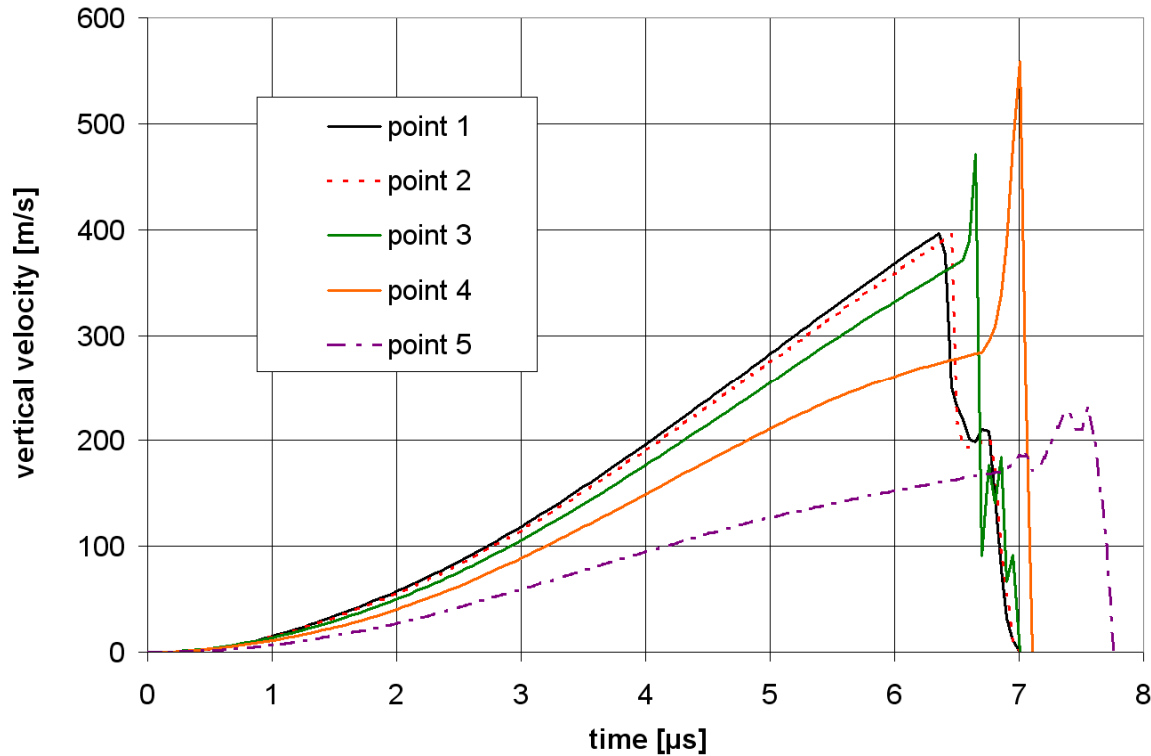


Fig. 3: Time versus velocity curves for five points during the impact of the contact partners. For point location see fig.2.

To analyze the influence of energy losses due to plastic yielding of the static contact partner, the same simulation is conducted, but the material of the static contact partner is steel S355. Thus, the plastic deformation of the stator and therewith the energy consumption is significantly decreased. The acceleration for contact point 3 & 4 is increased. This acceleration is possible because of lower energy consumption for plastic yielding of the static contact partner. However, the velocity of contact point 5 is decreased, see table 2. The velocity decrease of point 5 is subjected to higher energy consumption for acceleration of point 4.

| Point # | Vertical velocity EN AW 6060 stator | Vertical velocity steel s355 stator |
|---------|-------------------------------------|-------------------------------------|
| 1       | 396                                 | 396                                 |
| 2       | 395                                 | 395                                 |
| 3       | 471                                 | 513                                 |
| 4       | 558                                 | 628                                 |
| 5       | 230                                 | 197                                 |

Table 2: Vertical velocities for five points in the weld zone. Comparison for static contact partner made of Aluminum and Steel.

Given a sufficient ratio between contact normal stress and contact tangential stress, a bow wave builds up within the interfacial zone (see fig. 4). This results in extreme deformations in a small zone neighboring the contact faces. The zone of plastic straining measures only some micrometers

in thickness, however this is sufficient to crack up the oxide layers. Hence, metallic pure and therewith highly reactive surfaces contact each other under high contact normal pressure, a metallic bond is established. Fig. 4 illustrates the deformation of the interfacial zone. The sinusoidal line represents the welding seam. Grain deformation shows that impact direction was from left to right. The grain size is not increased with respect to the initial grain size of the material, i.e. there is no grain growth caused by heat, like in fusion welding processes.

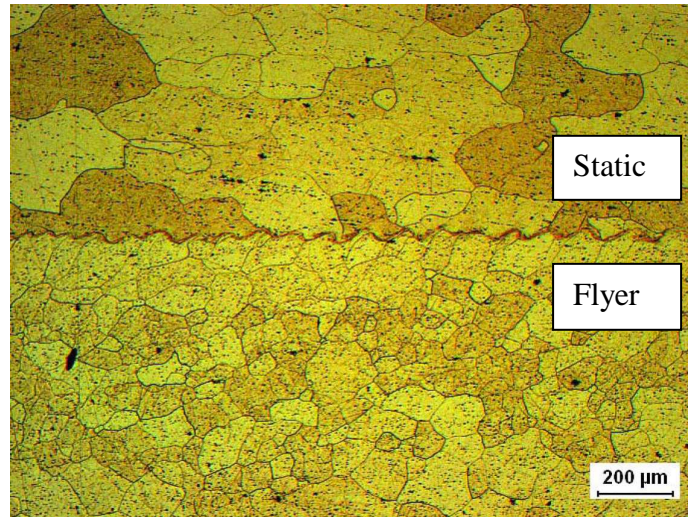


Fig. 4: Microsection of an EMPT welding

### Properties of an EMPT weld

EMPT sheet welding provides possibility to weld metals of different melting temperature together, because no heat is implemented into the material. However, in a small layer of 10-20μm thickness near the interface between both contact partners flash temperatures can be computed with the help of adiabatic Finite Element Analysis (FEA). The flash temperatures are caused by the severe plastic deformation of the interfacial zone. The temperature peak within this small zone can be several 100°C, but thermal conductivity decreases the temperature within very short time. Hence, no changes of the metal microstructure can be identified.

To analyze the strength of the welding seam, shear tests are conducted. To ensure pure shear, the specimen is an assembly of three parts. Two parts lying in a common plane are connected by a third sheet with the help of two EMPT overlap welds (fig.5).

Three different failure patterns are identified:

1. Failure of the weaker material near the welding seam (Fig. 5: 1mm Al – 1mm Cu)
2. Shear failure of the welding seam (Fig. 5: 2mm Al – 2mm steel)
3. Delamination of the zinc coating (Fig. 5: 1mm Al – 1.5mm zinc coated Trip steel)

The first failure mode, cracking near the welding seam, is mainly due to a small reduction in wall thickness of the flyer, which is caused by the magnetic pressure loading within the flyer acceleration (see fig. 2,  $t_1$ ). This notch represents the weakest point of the tensile test specimen.

The second failure mode, shearing of the welding seam, becomes dominant when the welding seam area is smaller than the cross sectional area of the tensile test specimen. These both failure modes indicate that the strength of an EMPT weld can be estimated by multiplying the shear strength of the weaker material by the area of the welding seam. Detailed analysis of the failure modes will be published in next future.

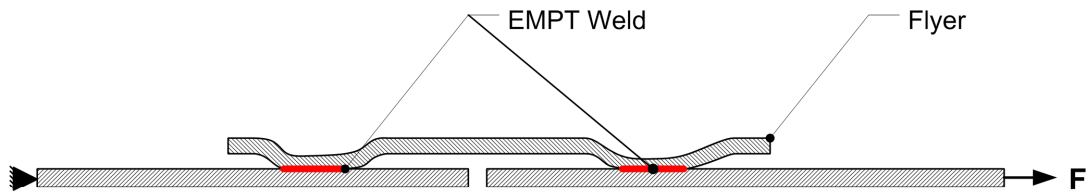


Fig. 5: EMPT welded tensile test specimen (25.11.2010)

Welding on zinc coated steel is possible; however in this case, the strength of the weld is dominated by the adhesion of the zinc on the steel. Micrographs are made for analysis of the welding zone. No failure of the zinc coating during the welding process is found see fig. 6, 1<sup>st</sup> line, left. However, the zinc coating delaminates during shear testing of the weld (Fig 5, right and Fig 6, 1<sup>st</sup> line, right). Energy dispersive X-ray spectroscopy (EDX) analysis proves the delamination of the zinc coating, see fig 6, 2<sup>nd</sup> line right. After failure of the welding seam, in the area of the cracked welding seam a homogeneous zinc coating is found on both joint partners (see fig. 6, 2<sup>nd</sup> line)

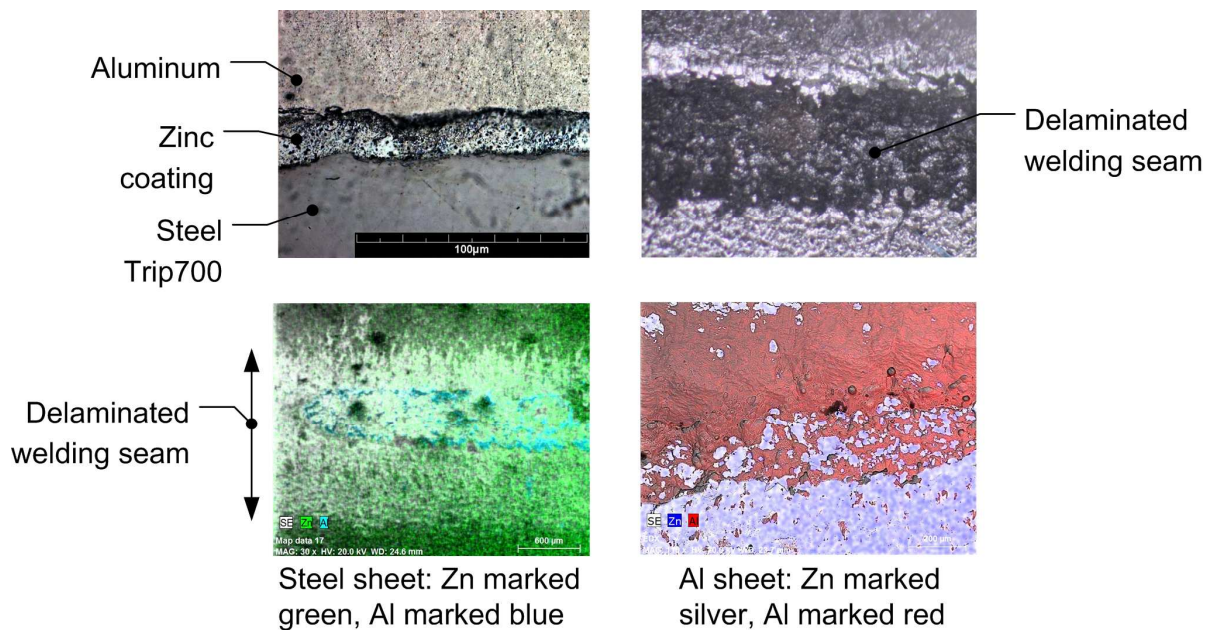


Fig. 6: Microsection of an EMPT weld Aluminum to zinc coated steel TRIP 700 and analysis of the tensile test specimen failure

## Samples

EMPT welding is capable for production of welds between dissimilar sheet metals. Here, joints which are not accomplishable by fusion welding processes can be manufactured, for example aluminum-steel welds. Fig. 7 represents an overview of materials welded. Moreover, welding thin sheet metals on very thick workpieces is possible, see also fig. 7. Fig. 8 illustrates an additional sample of 500 mm weld length done within one pulse. The welding velocity is dominated by the time essential to charge the capacitors of the pulse generator. For the 500 mm weld length per pulse at present 12 seconds charging time is mandatory. This results in an effective welding velocity of 2.5 m/minute. Objective of current work is the further increase of the welding velocity.

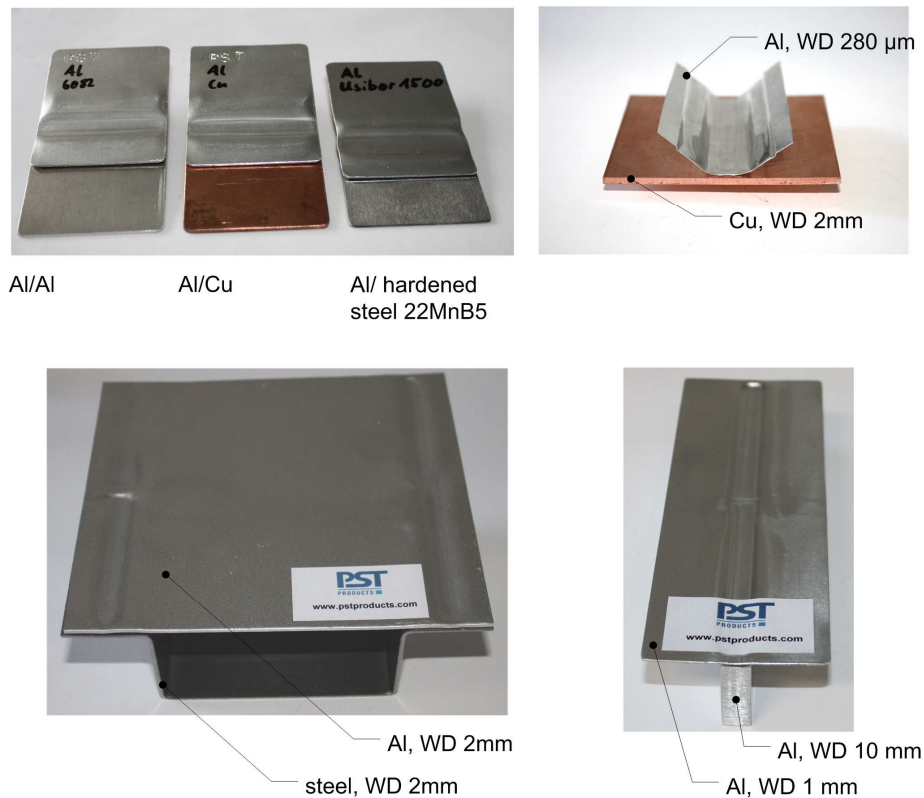


Fig. 7: EMPT welded samples of dissimilar metals respectively high wall thickness gradients (25.11.2010).



Fig. 8: Al- Al sample 450 mm weld length (25.11.2010)

## Summary

The electromagnetic pulse technology provides possibility for material hybrid sheet metal welding. For example aluminum to steel sheet welding is possible. This technique is adiabatic, i.e. no external thermal energy is brought in the workpiece material. Hence, no micro-structural changes caused by heat are found (no heat affected zone, no grain growth, no strength losses). The strength of the weld is approximately the shear strength of the weaker material of both contact partners multiplied by the weld seam area. At present welding length of up to 500 mm per pulse is possible. At a pulse repetition rate of five per minute, a welding velocity of 2.5 m/ minute is possible. Objective of current work is the further increase of the welding velocity.

## References

- [1] L.F. Mondolfo: *Aluminum alloys: Structure and properties*. Butterwoth (1976)
- [2] N. Janck, H. Stauffer, J. Bruckner: *Schweißverbindungen von Stahl mit Aluminium- Eine Perspektive für die Zukunft*. BHM Berg- und Hüttenmännische Monatshefte Volume 153, Number 5, pp. 189-192 (2008)
- [3] G. Aichele. Verschweißen von Aluminium mit Stahl. *Industriebedarf* 5-6, 2008, pp. 14-16 (2008)
- [4] A. Oosterkamp, L. Oosterkamp, A. Nordeide: *Kissing bond phenomena in solid state welding of aluminum alloys*. *Welding Journal* 83(8), pp.225-231 (2004)
- [5] C.B. Smith, W. Crusan, et.al.: *Friction stir welding in the automotive industry*. <http://www.frictionstirlink.com/publications/Pub07FSWAutoIndTMSPaperpdf.pdf>
- [6] M.K. Kazimierzciuk: *High frequency magnetic components*. Wiley (2009)